



CHORUS

This is the accepted manuscript made available via CHORUS. The article has been published as:

## Mesoscopic Rydberg Impurity in an Atomic Quantum Gas

Richard Schmidt, H. R. Sadeghpour, and E. Demler

Phys. Rev. Lett. **116**, 105302 — Published 10 March 2016

DOI: [10.1103/PhysRevLett.116.105302](https://doi.org/10.1103/PhysRevLett.116.105302)

# A mesoscopic Rydberg impurity in an atomic quantum gas

Richard Schmidt,<sup>1,2</sup> H. R. Sadeghpour,<sup>1</sup> and E. Demler<sup>2</sup>

<sup>1</sup>*ITAMP, Harvard-Smithsonian Center for Astrophysics, Cambridge MA 02138, USA*

<sup>2</sup>*Department of Physics, Harvard University, Cambridge MA 02138, USA*

Giant impurity excitations are powerful probes for exploring new regimes of far out of equilibrium dynamics in few- and many-body quantum systems, and *in-situ* observations of correlations. Motivated by recent experimental progress in spectroscopic studies of Rydberg excitations in ultracold atoms, we develop a new theoretical approach for describing multiscale dynamics of Rydberg excitations in quantum Bose gases. We find that the crossover from few- to many-body dynamics manifests in a dramatic change in spectral profile from resolved molecular lines to broad Gaussian distributions representing a superpolaronic state in which many atoms bind to the Rydberg impurity. We discuss signatures of this crossover in the temperature and density dependence of the spectra.

*Introduction.*— Until recently the main motivation for studying impurity dynamics came from the study of electron transport in mesoscopic and nano-electronic systems [1–4]. Theoretical work focused almost exclusively on fermionic systems [5, 6] discussing such spectacular phenomena as the Kondo effect [7, 8] and the orthogonality catastrophe [9–11]. In contrast, studies of impurities in bosonic systems were limited to equilibrium properties such as the polaron energy and effective mass [12–14]. However, recent efforts to probe non-equilibrium polaronic dynamics in bosonic gases have renewed theoretical interest [15–21].

The realization of Rydberg impurities in ultracold quantum gases [22–24] presents a new frontier where microscopic atomic physics meets condensed matter and mesoscopic physics, going beyond quantum simulations of strongly correlated states [25]. At high principal quantum numbers, Rydberg blockade ensures that only one excitation is possible [26–28], promoting the Rydberg atom to a novel realization of an impurity problem. At the same time Rydberg excitations in ultracold gases are predicted to form exotic molecular bound states [29, 30]. Their mesoscopic size with yet large binding energies, represent a multiscale challenge in impurity physics, requiring the confluence of powerful theoretical tools, from atomic and condensed matter physics.

In this work, we address the challenge of non-equilibrium dynamics of Bose polarons arising from Rydberg impurities and demonstrate how their dynamics manifests itself in the absorption spectra. Our approach employs microscopic molecular potentials calculated from Rydberg wave functions [31]. Using exact bound and scattering solutions, we solve the full time evolution of the many-body density matrix, based on a novel functional determinant approach (FDA) to bosonic systems. We show in de-

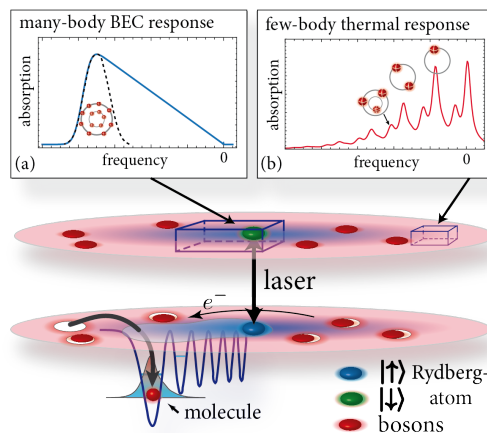


FIG. 1. When a Rydberg impurity is excited in a Bose gas, a molecular potential supporting ultra long-range vibrational states is formed. In a thermal gas these states are observed as few-body absorption lines (dimer, trimer, tetramer, etc.). The occupation of vibrational modes results in a shell structure as illustrated in (b). Deep in the condensed gas, the spectrum becomes Gaussian [dashed curve in (a)] representing a superpolaronic state. In typical experiments density averaged spectra [blue curve in (a)] are observed.

tail how few-body molecular lines at low densities evolve into a Gaussian profile at  $T=0$  in a Bose-Einstein condensate (BEC) signifying the formation of a giant superpolaronic state at higher densities. This dressed impurity state is comprised of a mesoscopic number of bound atoms and exhibits a shell structure in real space, see Fig. 1.

The present method applies generally to thermal and degenerate gases, is readily extendable to fermionic mixed-species systems, and allows to predict a wide range of time-dependent observables such as spin echo or Ramsey signals.

*Model for Rydberg impurities.*— We investigate a single Rydberg impurity immersed in a Bose gas of ultracold atoms, localized in space at arbitrary temperature  $T$  and particle density  $\rho$ . The Rydberg atom is initially in its electronic ground state,  $|\downarrow\rangle$ . In a two-photon laser excitation, the atom is transferred to an excited state,  $|\uparrow\rangle = |ns\rangle$ , of principal quantum number  $n$ , and whose orbital  $\psi_e(\mathbf{r})$  has a size comparable to the interparticle distance  $\rho^{-1/3}$ . The scattering of the Rydberg electron from the surrounding ground state atoms is described by the Fermi pseudopotential [32]. A host atom situated at a distance  $\mathbf{r}$  from the impurity ion core at  $\mathbf{R} = 0$  is then subject to the potential [23]

$$V_{\text{Ryd}}(\mathbf{r}) = \frac{2\pi\hbar a_e}{m_e} |\psi_e(\mathbf{r})|^2. \quad (1)$$

This Born-Oppenheimer potential supports bound vibrational states [29], when the Rydberg-electron perturber-atom scattering length  $a_e$  is negative; cf. Fig. 1.

The main knob for the control of interactions in quantum gases has universally been the zero-momentum scattering length which can be manipulated by magnetic or optical Fano-Feshbach spectroscopy [33]. In Rydberg impurity excitations, it is the variation of  $|\psi_e(\mathbf{r})|^2$  which brings in the possibility to probe the quantum gas in a completely novel way, i.e. by changing  $n$ .

Theoretical analysis of Rydberg molecule excitations [34–37] have thus far relied on few-body atomic methods, which by construction cannot account for many-body quantum dynamics. In contrast, to describe the physics on all length scales, arbitrary temperature and density, one must rigorously include the full quantum statistics, encoded in the many-body density matrix. This applies in particular to high Rydberg excitations where the ultracold medium is probed on mesoscopic length scales and standard many-body techniques such as mean-field or variational approaches fail due to the multiscale and non-perturbative character of the underlying microscopic physics.

To this end, we study the dynamics of the Rydberg impurity governed by the many-body Hamiltonian

$$\hat{H} = \sum_{\mathbf{k}} \epsilon_{\mathbf{k}} \hat{b}_{\mathbf{k}}^\dagger \hat{b}_{\mathbf{k}} + \sum_{\mathbf{q}} V(\mathbf{q}) \hat{b}_{\mathbf{k}+\mathbf{q}}^\dagger \hat{b}_{\mathbf{k}} |\uparrow\rangle \langle\uparrow| \quad (2)$$

where  $\hat{b}_{\mathbf{k}}^\dagger$ ,  $\hat{b}_{\mathbf{k}}$  represent the creation and annihilation operators of the bath bosons of mass  $m$ , momentum  $\mathbf{k}$ ,  $\epsilon_{\mathbf{k}} = \mathbf{k}^2/2m$ , and  $V(\mathbf{q})$  is the Fourier transform of Eq. (1). The Fock space is constructed from the bosonic single-particle orbitals, obtained

from the bound and continuum eigensolutions of the Schroedinger equation for a localized Rydberg impurity with infinite mass. The scattering length in the pseudopotential in Eq. (1) is rescaled to reproduce the bound molecular dimer energies. Since the Rydberg molecule formation takes place on time scales of the vibrational energies, the Rydberg ion recoil can be ignored. Since this time is short compared to the time for collective bath excitations, the inter-boson interaction can be neglected as well.

*Rydberg impurity spectra from a quantum quench problem.*— We compute the time-dependent overlap

$$S(t) = \text{tr}[e^{i\hat{H}_0 t} e^{-i\hat{H} t} \hat{\rho}] \quad (3)$$

where  $\hat{\rho}$  is the density matrix representing the initial state of the system, and  $\hat{H}_0$  is the Hamiltonian in the absence of the impurity. The expression (3) describes the many-body dephasing dynamics following the sudden quench of the Rydberg potential and can be directly measured using Ramsey spectroscopy [38–41]. The Fourier transform of Eq. (3) yields the two-photon absorption spectrum  $A(\omega) = 2 \text{Re} \int_0^\infty dt e^{i\omega t} S(t)$  [39, 42].

*Zero temperature description.*— We focus first on a Bose gas at  $T = 0$ . The Fock state representing the atoms in a BEC is given by  $|\Psi_0\rangle = 1/\sqrt{N!} (\hat{b}_0^\dagger)^N |\text{vac}\rangle$  where  $N$  is the particle number. The time-dependent overlap (3) is then evaluated with respect to the density matrix  $\hat{\rho}_{\text{BEC}} = |\Psi_0\rangle \langle\Psi_0|$  and gives

$$S_{\text{BEC}}(t) = \left( \sum_{\alpha} |\langle\alpha|s\rangle|^2 e^{i(\epsilon_s - \omega_\alpha)t} \right)^N, \quad (4)$$

where the collective index  $\alpha = (k, l, m)$  labels the interacting single particle states  $|\alpha\rangle$  with nodal number  $k$ , angular momentum  $l$  of projection  $m$  and energy  $\omega_\alpha$ . The lowest non-interacting scattering state is  $|s\rangle = \hat{b}_0^\dagger |\text{vac}\rangle$  with energy  $\epsilon_s$ .

We demonstrate the utility of our method for excitations in a  $^{87}\text{Rb}$  gas, as recently realized [23, 24, 30], by focussing on excitations into Rb(71s). Vibrational bound and scattering states up to large angular momenta are calculated in a spherical box of radius  $10 \mu\text{m}$  [43]. We incorporate the finite length  $\tau_p$  of excitation pulses in Eq. (3), and the finite lifetime of Rydberg excitations [44] can be included as well.

In Fig. 2 we show the absorption spectrum for a Rydberg excitation in the BEC phase at  $T=0$ , for different densities  $\rho_0 = \rho(\mathbf{r} = 0)$ . The low density response is shown in Fig. 2(a). Here the interparticle

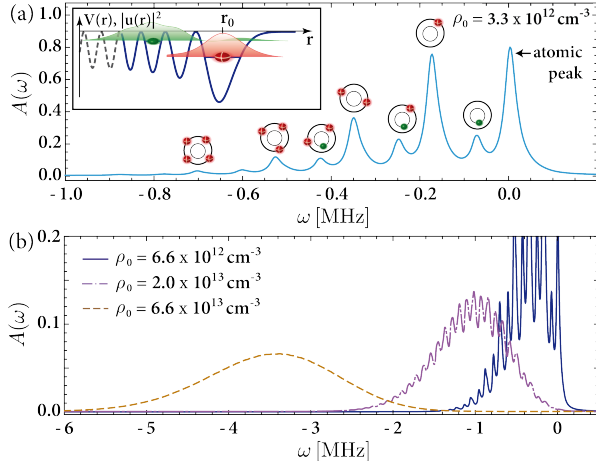


FIG. 2. Absorption spectrum at  $T = 0$  for a Rydberg excitation to  $^{87}\text{Rb}(71s)$  ( $\tau_p = 50\mu\text{s}$ ). (a) Low density  $\rho_0 = 3.3 \times 10^{12}\text{cm}^{-3}$ . The circles with spheres above the peaks represent atoms bound in different orbitals. Inset: Occupation probability  $|u(r)|^2$  for s-wave single-particle states. (b) Crossover to the many-body regime with increasing densities.

spacing exceeds the range of the Rydberg potential,  $r_0 \approx 8650 a_0$ . The physics is dominated by few-body interactions resulting in a series of molecular lines corresponding to one, two or more medium atoms bound and localized inside the Rydberg orbit. These molecular lines were recently observed in a thermal Rb gas [23, 30], and are identified in Fig. 2(a) with a red sphere for the fundamental dimer line, with two red spheres for the associated trimer line, and similarly for the tetramer and pentamer lines.

The Rydberg potential Eq. (1) supports several vibrational bound states. This leads to additional spectral features represented by a combination of green and red spheres, which are associated with exotic bound dimers, trimers, tetramers, etc. The single-boson wavefunctions [see inset in Fig. 2(a)] reveal that atoms in the first excited vibrational orbit are localized at smaller distances from the Rydberg ion. As a consequence these complex molecules exhibit a spatial structure reminiscent of the shell model in nuclear physics [45].

As the density is increased, c.f. Fig. 2(b), we predict a crossover from resolved molecular lines with asymmetric envelopes (blue and purple lines) to a Gaussian profile (brown line) whose peak moves progressively to larger detunings with increasing density. This broad spectral response corresponds to the formation of a superpolaron comprised of a large number of bound atoms. Its emergence is rooted in the stochastic occupation of densely packed many-

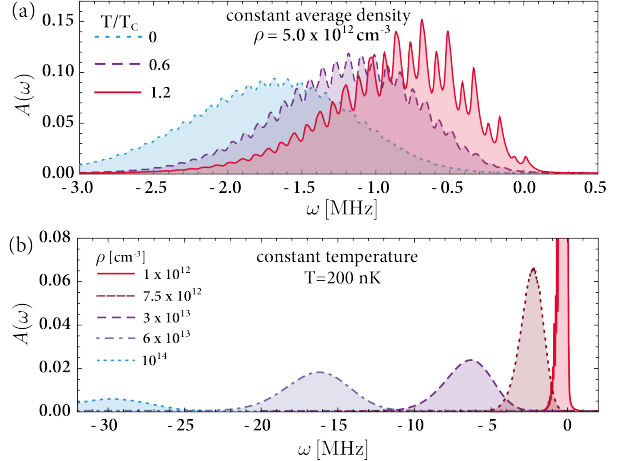


FIG. 3. Temperature and density dependent absorption spectrum ( $\tau_p = 50\mu\text{s}$ ). (a) Spectral dependence on the temperature at fixed density  $\rho$ . (b) Absorption spectrum at fixed temperature for different average densities of the Bose gas. These spectra can be observed in experiments with crossed narrow-beam lasers [24, 37].

body states absent in typical realizations of impurity problems [46–48].

The predicted Gaussian profile can be understood from the spectral decomposition of  $A(\omega)$ , in excitations from the BEC ground state  $|\Psi_0\rangle$  into interacting single-particle states  $|\alpha_i\rangle$  [43]. The resulting multinomial distribution is dominated by a few states with favorable Franck-Condon factors  $p_i = |\langle\alpha_i|s\rangle|^2$ . If only the deepest bound state  $|B\rangle$  and the zero-energy scattering state  $|\tilde{s}\rangle$  are considered, a binomial distribution results [43],

$$A(\omega) = \sum_{m=1}^N \binom{N}{m} p^m (1-p)^{N-m} \delta(\omega - m\epsilon_B). \quad (5)$$

Here  $p = |\langle B|s\rangle|^2$  is the probability to transfer a BEC atom from the single-particle state  $|s\rangle$  into the bound state. For large particle number  $N$ , this distribution evolves into a Gaussian. In the exact spectrum shown in Fig. 2 additional interacting states contribute, leading to a multinomial spectral decomposition of  $A(\omega)$  which also evolves into a Gaussian. We emphasize that the Gaussian distribution emerges solely due to the canonical nature of atomic BEC and will be absent in a grand-canonical BEC such as recently realized using dye filled cavities [49].

*Finite temperature description.*— At finite temperatures, the gas is composed of  $N_0$  condensed and  $N'$  thermally depleted atoms. In order to account for their quantum statistics, we make use of a novel

bosonic FDA, based on earlier work on fermionic systems [50, 51]; see also [52] where bosonic systems are briefly discussed.

Our method applies generally to impurities interacting with a bosonic environment. In its original formulation [50–52], the FDA dealt with many-body systems which are described by a grand-canonical ensemble, such as fermions with fixed particle number or bosons in a thermal cloud. However, a BEC of atoms cannot be described within the grand-canonical approach [53].

We take this into account by treating the thermal cloud and the condensate as separate subsystems leading to

$$S(t) = S_{\text{BEC}}(t) \times S_{\text{th}}(t), \quad (6)$$

where  $S_{\text{BEC}}(t)$  and  $S_{\text{th}}(t)$  refer to the time-dependent overlaps of the condensate and the thermal cloud, respectively. The expression (6) becomes exact in the limits  $T/T_c \ll 1$  and  $T/T_c \gg 1$ , where  $T_c$  is the condensate transition temperature.

In general, many-body traces as in Eq. (3), are difficult to evaluate due to the exponential size of Hilbert space. However, making use of the FDA, the thermal contribution can be expressed as [52]

$$S_{\text{th}}(t) = \det \left[ 1 + \hat{n} - \hat{n} e^{i\hat{h}_0 t} e^{-i\hat{h} t} \right]^{-1}. \quad (7)$$

Here  $\hat{n} = 1/[e^{\beta(\hat{h}_0 - \mu)} - 1]$  denotes the single particle occupation number operator,  $\mu$  is the chemical potential and  $\beta = 1/k_B T$  with  $k_B$  the Boltzmann constant. The operators  $\hat{h}$ ,  $\hat{h}_0$  are the single-particle counterparts of  $\hat{H}$  and  $\hat{H}_0$ . Eq. (7) allows for an efficient transform of the many-body trace into a determinant in single-particle space. In Fig. 3(a) we show the temperature dependence of the absorption spectrum at fixed density  $\rho$ . With increasing temperature, the Gaussian profile at  $T = 0$  (dotted line) morphs into an asymmetric profile with resolved dimer, trimer, . . . lines. These molecular lines differ from the few-body spectra [cf. Fig. 2] due to dressing by many-body fluctuations.

In contrast, in Fig. 3(b), the temperature is fixed. At low densities (solid line) the gas is purely thermal and molecular lines are observed at low detunings (note the frequency scales in Fig. 3). As the density is increased and the gas condenses, the spectrum evolves from an asymmetric form to a Gaussian profile located at a detuning corresponding to binding of hundreds of atoms within the Rydberg electron orbit.

*Experimental realization.*— In experiments [23, 24, 36, 37], atomic clouds have inhomogeneous density profiles and are probed by lasers of finite waist.

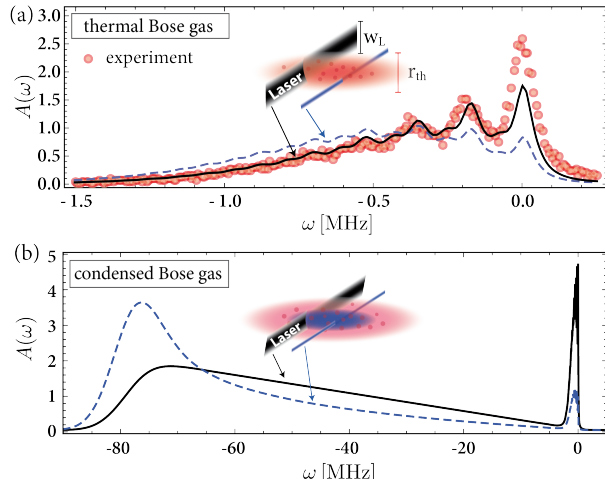


FIG. 4. Density averaged absorption spectra for Rb(71s) excitations ( $\tau_p = 30\mu\text{s}$ ). (a) Thermal gas at  $T = 500\text{ nK}$  and trap center density  $\rho_0 = 1.7 \times 10^{12}\text{ cm}^{-3}$ . Results are shown for a laser profile illuminating the cloud over the full cylindrical radius  $r_{\text{th}}$  (black) and for a laser of small waist (dashed, blue). For illustration the data reported in Gaj *et al.* [23, 54] is shown as red dots. (b) Density averaged absorption spectrum at  $T/T_c = 0.47$  for a partially condensed gas of (zero temperature) peak density  $\rho_p = 2.3 \times 10^{14}\text{ cm}^{-3}$ .

In Fig. 4 we present Rydberg spectra that take into account these density inhomogeneities using a local density approximation (LDA). The analysis is done for realistic trap parameters, temperatures, densities, and Rb-Rb scattering length [43]. We assume a Thomas-Fermi profile for the condensate fraction, and the thermal fraction is treated within the Hartree-Fock approximation [55].

In Fig. 4(a), the averaged spectra for two laser profiles are shown. The solid line represents a laser which excites the cloud along its full radial extent while the dashed line corresponds to a laser of a narrow waist. The LDA leads to an asymmetric line shape with a long tail and molecular oligomer lines. For a laser of small waist, we predict a shift of spectral response to deeper detunings. We emphasize that these calculations are performed without any adjustable parameters, except for the finite length of the laser pulse. For illustration we compare our theoretical calculations to the molecular spectrum for  $^{87}\text{Rb}(71\text{s})$  observed by Gaj *et al.* [23].

In Fig. 4(b), we present the density averaged absorption spectra at  $T/T_c < 1$  [43]. The response predicted in Fig. 4(b) results from the average over Gaussian (superpolaronic) distributions measured at different densities. While the response of the condensed atoms leads to a broad shoulder at large de-

tunings, the thermal atoms contribute at small detunings.

In recent experiments on Rydberg impurity excitations in a  $^{87}\text{Rb}$  BEC [24, 37], such LDA profiles were interpreted using a classical description of atoms inside the Rydberg orbit, whose detunings were calculated from a combined s- and p-wave scattering of the Rydberg electron from the ground state atoms. Such a classical approach does not account for quantum many-body effects.

In an ultracold strontium gas [36], p-wave scattering leads to binding, while in alkali metal atoms this scattering is resonant. Therefore trapped Sr represents a pristine probe of quantum many-body effects and molecular shell structure.

*Summary and Outlook.*— We present a novel many-body formalism for analyzing the non-equilibrium time evolution of Bose gases interacting with spatially extended impurities. We demonstrate that spectroscopy of Rydberg excitations allows for probing this dynamics in a new parameter regime where the impurity itself extends over the entire system. From the Fourier analysis of the time-resolved overlaps we find qualitative changes with temperature and density reflecting different dynamical regimes. At low densities the existence of a molecular shell structure is found and the emergence of a metastable superpolaronic state at large densities and low temperatures is predicted.

Rydberg excitations in fermionic gases are another exciting opportunity for exploring impurity dynamics on mesoscopic scales, for which the FDA is ideally suited [39–41]. It remains an open question whether Pauli blocking is observable resulting in a molecular shell structure similar to that in nuclear physics. Our approach allows for efficient real time evolution of occupation numbers, *in situ* density, and correlation functions. These can be probed, for instance, in experiments aiming at direct observation of shell structure, and the study of locally controlled heating of ultracold gases by Rydberg impurities. The coherence of Rydberg excitations is paramount for their application in quantum information processing [23, 56, 57]. Our approach can investigate density dependent dephasing as a fundamental limit on entangled state preparation.

*Acknowledgements.*— R. S. and H. R. S. were supported by the NSF through a grant for the Institute for Theoretical Atomic, Molecular, and Optical Physics at Harvard University and the Smithsonian Astrophysical Observatory. E. D. acknowledges support from Harvard-MIT CUA, NSF Grant No. DMR-1308435, AFOSR Quantum Simulation MURI, the ARO-MURI on Atomtronics, and support from Dr. Max Rössler, the Walter Haefner Foundation, the ETH Foundation, and the Simons Foundation. We are thankful to A. Gaj and T. Pfau for providing data.

- 
- [1] P. A. Lee and T. V. Ramakrishnan, *Rev. Mod. Phys.* **57**, 287 (1985).
  - [2] W. G. van der Wiel, S. De Franceschi, J. M. Elzerman, T. Fujisawa, S. Tarucha, and L. P. Kouwenhoven, *Rev. Mod. Phys.* **75**, 1 (2002).
  - [3] C. Beenakker, in *Proceedings of the International School of Physics Enrico Fermi*, Vol. 162 (IOS Press; Ohmsha; 1999, 2007) p. 307.
  - [4] H. Haug, A.-P. Jauho, and M. Cardona, *Quantum kinetics in transport and optics of semiconductors*, Vol. 2 (Springer, 2008).
  - [5] N. Prokof'ev and B. Svistunov, *Phys. Rev. B* **77**, 020408 (2008).
  - [6] F. Chevy and C. Mora, *Reports on Progress in Physics* **73**, 112401 (2010).
  - [7] A. C. Hewson, *The Kondo problem to heavy fermions*, Vol. 2 (Cambridge university press, 1997).
  - [8] D. Goldhaber-Gordon, H. Shtrikman, D. Mahalu, D. Abusch-Magder, U. Meirav, and M. A. Kastner, *Nature* **391**, 156 (1998).
  - [9] P. W. Anderson, *Phys. Rev. Lett.* **18**, 1049 (1967).
  - [10] P. Nozières, P.ères and C. T. De Dominicis, *Phys. Rev.* **178**, 1097 (1969).
  - [11] A. Rosch, *Advances in Physics* **48**, 295 (1999).
  - [12] R. M. Kalas and D. Blume, *Phys. Rev. A* **73**, 043608 (2006).
  - [13] J. T. Devreese and A. S. Alexandrov, *Reports on Progress in Physics* **72**, 066501 (2009).
  - [14] Y. E. Shchadilova, F. Grusdt, A. N. Rubtsov, and E. Demler, arXiv preprint arXiv:1410.5691 (2014).
  - [15] S. P. Rath and R. Schmidt, *Phys. Rev. A* **88**, 053632 (2013).
  - [16] R. Scelle, T. Rentrop, A. Trautmann, T. Schuster, and M. K. Oberthaler, *Phys. Rev. Lett.* **111**, 070401 (2013).
  - [17] A. Shashi, F. Grusdt, D. A. Abanin, and E. Demler, *Phys. Rev. A* **89**, 053617 (2014).
  - [18] L. A. P. Ardila and S. Giorgini, *Phys. Rev. A* **92**, 033612 (2015).
  - [19] J. Wang, M. Gacesa, and R. Côté, *Phys. Rev. Lett.* **114**, 243003 (2015).
  - [20] R. Schmidt and M. Lemeshko, *Phys. Rev. Lett.* **114**, 203001 (2015).
  - [21] R. Schmidt and M. Lemeshko, *Phys. Rev. X* **6**, 011012 (2016).
  - [22] J. B. Balewski, A. T. Krupp, A. Gaj, D. Peter, H. P.

- Buchler, R. Low, S. Hofferberth, and T. Pfau, *Nature* **502**, 664 (2013).
- [23] A. Gaj, A. T. Krupp, J. B. Balewski, R. Löw, S. Hofferberth, and T. Pfau, *Nat Commun* **5** (2014).
- [24] H. Nguyen, T. C. Liebisch, M. Schlagmüller, G. Lochead, K. M. Westphal, R. Löw, S. Hofferberth, and T. Pfau, arXiv preprint arXiv:1506.05302 (2015).
- [25] I. Bloch, J. Dalibard, and S. Nascimbene, *Nat Phys* **8**, 267 (2012).
- [26] I. Mourachko, D. Comparat, F. de Tomasi, A. Fioretti, P. Nosbaum, V. M. Akulin, and P. Pillet, *Phys. Rev. Lett.* **80**, 253 (1998).
- [27] A. Gaetan, Y. Miroshnychenko, T. Wilk, A. Chotia, M. Viteau, D. Comparat, P. Pillet, A. Browaeys, and P. Grangier, *Nat Phys* **5**, 115 (2009).
- [28] E. Urban, T. A. Johnson, T. Henage, L. Isenhower, D. D. Yavuz, T. G. Walker, and M. Saffman, *Nat Phys* **5**, 110 (2009).
- [29] C. H. Greene, A. S. Dickinson, and H. R. Sadeghpour, *Phys. Rev. Lett.* **85**, 2458 (2000).
- [30] V. Bendkowsky, B. Butscher, J. Nipper, J. P. Shaffer, R. Low, and T. Pfau, *Nature* **458**, 1005 (2009).
- [31] M. Marinescu, H. R. Sadeghpour, and A. Dalgarno, *Phys. Rev. A* **49**, 982 (1994).
- [32] E. Fermi, *Il Nuovo Cimento* (1924-1942) **11**, 157 (1934).
- [33] C. Chin, R. Grimm, P. Julienne, and E. Tiesinga, *Rev. Mod. Phys.* **82**, 1225 (2010).
- [34] I. C. H. Liu and J. M. Rost, *The European Physical Journal D* **40**, 65 (2006).
- [35] V. Bendkowsky, B. Butscher, J. Nipper, J. B. Balewski, J. P. Shaffer, R. Löw, T. Pfau, W. Li, J. Stanojevic, T. Pohl, and J. M. Rost, *Phys. Rev. Lett.* **105**, 163201 (2010).
- [36] B. J. DeSalvo, J. A. Aman, F. B. Dunning, T. C. Killian, H. R. Sadeghpour, S. Yoshida, and J. Burgdörfer, *Phys. Rev. A* **92**, 031403 (2015).
- [37] M. Schlagmüller, T. C. Liebisch, H. Nguyen, G. Lochead, F. Engel, F. Böttcher, K. M. Westphal, K. S. Kleinbach, R. Löw, S. Hofferberth, T. Pfau, J. Pérez-Ríos, and C. H. Greene, *Phys. Rev. Lett.* **116**, 053001 (2016).
- [38] J. Goold, T. Fogarty, N. Lo Gullo, M. Paternostro, and T. Busch, *Phys. Rev. A* **84**, 063632 (2011).
- [39] M. Knap, A. Shashi, Y. Nishida, A. Imambekov, D. A. Abanin, and E. Demler, *Phys. Rev. X* **2**, 041020 (2012).
- [40] M. Cetina *et al.*, In prep.
- [41] R. Schmidt, H. Sadeghpour, and E. Demler, In prep.
- [42] G. D. Mahan, *Many-particle physics*, Physics of solids and liquids (Plenum, New York, NY, 1990).
- [43] See the supplemental material.
- [44] I. I. Beterov, I. I. Ryabtsev, D. B. Tretyakov, and V. M. Entin, *Phys. Rev. A* **79**, 052504 (2009).
- [45] J. M. Blatt and V. F. Weisskopf, *Theoretical nuclear physics* (Springer Science & Business Media, 2012).
- [46] A. Schirotzek, C. H. Wu, A. Sommer, and M. W. Zwierlein, *Phys. Rev. Lett.* **102**, 230402 (2009).
- [47] C. Kohstall, M. Zaccanti, M. Jag, A. Trenkwalder, P. Massignan, G. M. Bruun, F. Schreck, and R. Grimm, *Nature* **485**, 615 (2012).
- [48] C. Latta, F. Haupt, M. Hanl, A. Weichselbaum, M. Claassen, W. Wueter, P. Fallahi, S. Faelt, L. Glazman, J. von Delft, H. E. Tureci, and A. Imamoglu, *Nature* **474**, 627 (2011).
- [49] J. Schmitt, T. Damm, D. Dung, F. Vewinger, J. Klaers, and M. Weitz, *Phys. Rev. Lett.* **112**, 030401 (2014).
- [50] L. Levitov and G. Lesovik, *JETP Letters* **58**, 230 (1993).
- [51] L. S. Levitov, H. Lee, and G. B. Lesovik, *Journal of Mathematical Physics* **37**, 4845 (1996).
- [52] I. Klich (Kluwer, Dordrecht, 2003) pp. 397–402.
- [53] R. M. Ziff, G. E. Uhlenbeck, and M. Kac, *Physics Reports* **32**, 169 (1977).
- [54] A. Gaj, (2015), private communication.
- [55] L. P. Pitaevskii and S. Stringari, *Bose-Einstein Condensation* (Oxford: Clarendon, 2003).
- [56] M. Saffman, T. G. Walker, and K. Mølmer, *Rev. Mod. Phys.* **82**, 2313 (2010).
- [57] I. I. Beterov, M. Saffman, V. P. Zhukov, D. B. Tretyakov, V. M. Entin, E. A. Yakshina, I. I. Ryabtsev, C. W. Mansell, C. MacCormick, S. Bergamini, and M. P. Fedoruk, *Laser Physics* **24**, 074013 (2014).